Electronic Supplementary Information (ESI)

Sn(II) induced concentration dependent dynamic to static excimer conversion of a conjugated naphthalene derivative

Susanta Adhikari[a], Sandip Mandal[b], Avijit Ghosh[a], Subhajit Guria[a] and Debasis Das[b]**

[a]*Department of Chemistry, University of Calcutta, 92, A.P.C. Road, Kolkata 700 009, West Bengal, India.*
[b]*Department of Chemistry, The University of Burdwan, Burdwan 713104, West Bengal, India*

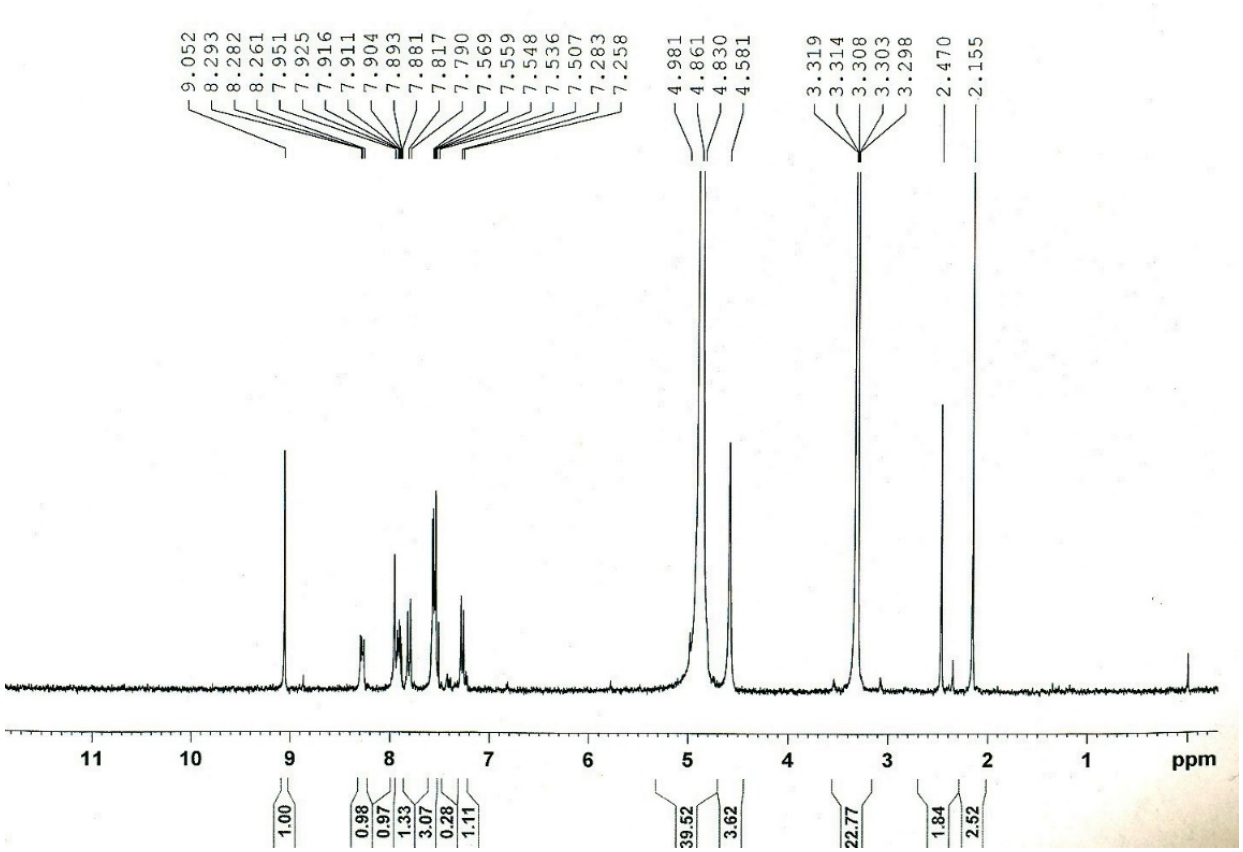

Figure S1 ^{1}H NMR spectrum of **L** in CD_3OD

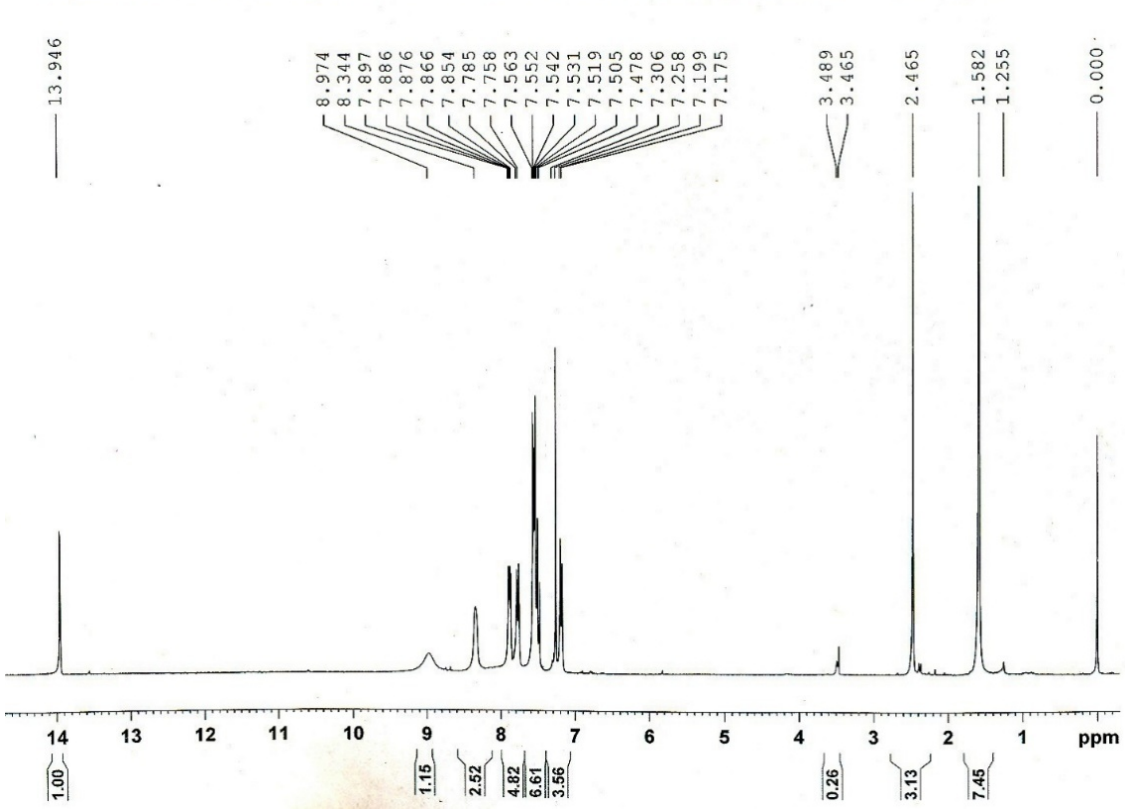

Figure S2 ^{1}H NMR spectrum of **L** in $CDCl_3$

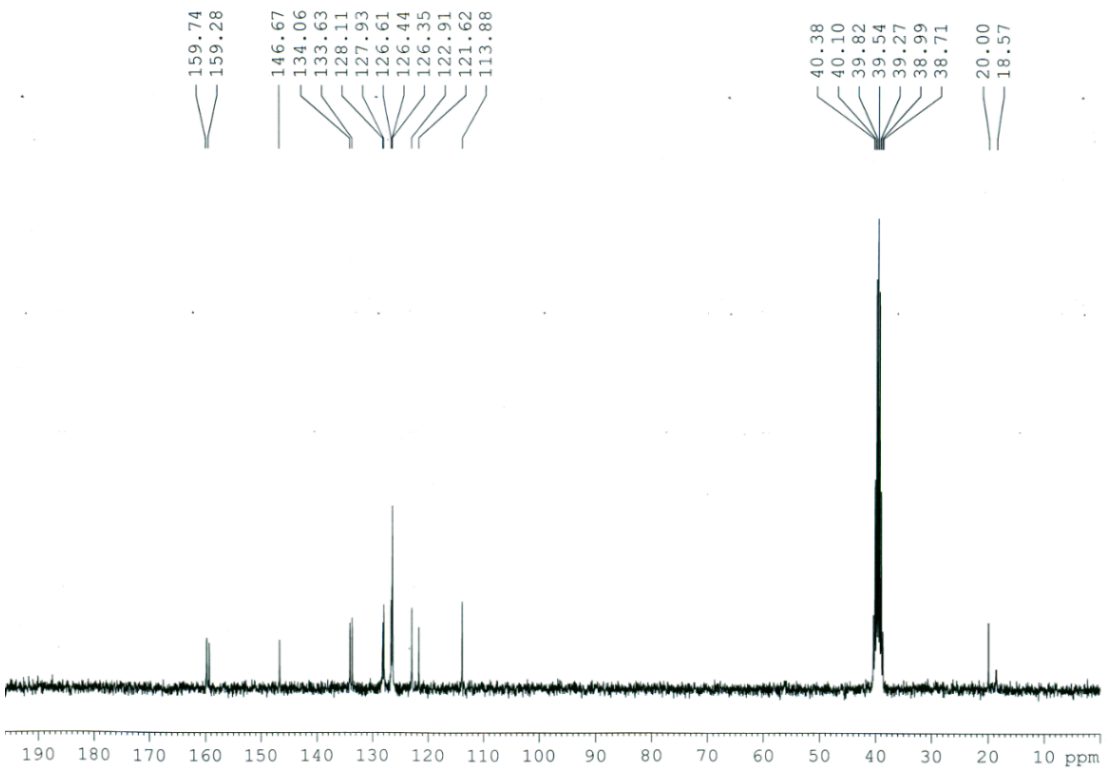

Figure S3^{13}C NMR spectrum of **L** in DMSO-d_6

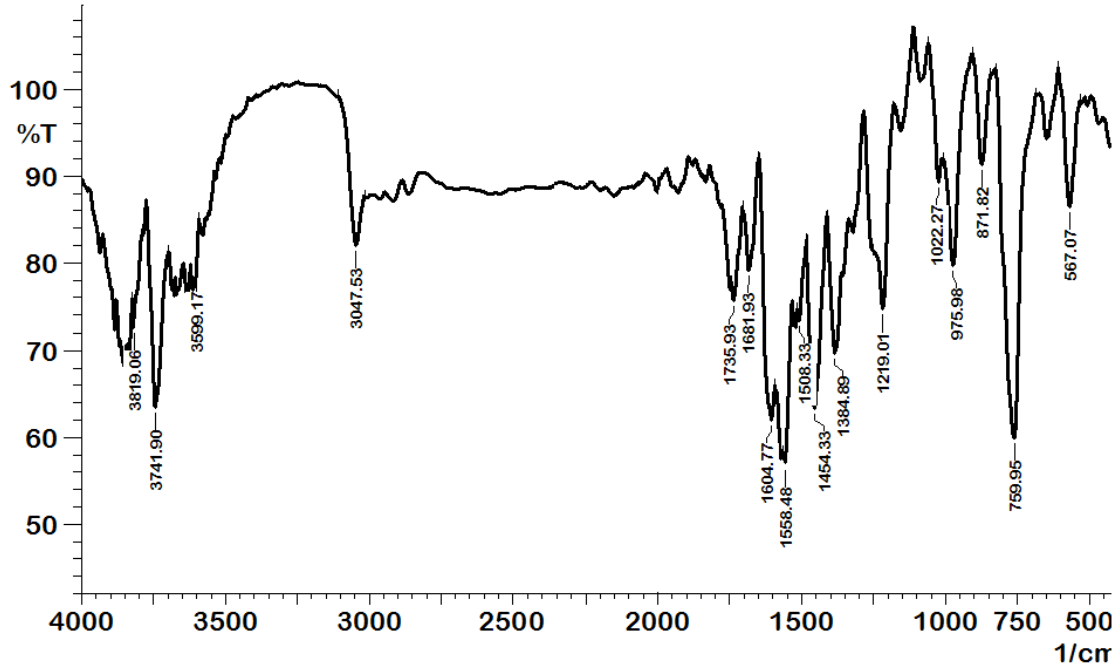

Figure S4. FTIR spectrum of **L**

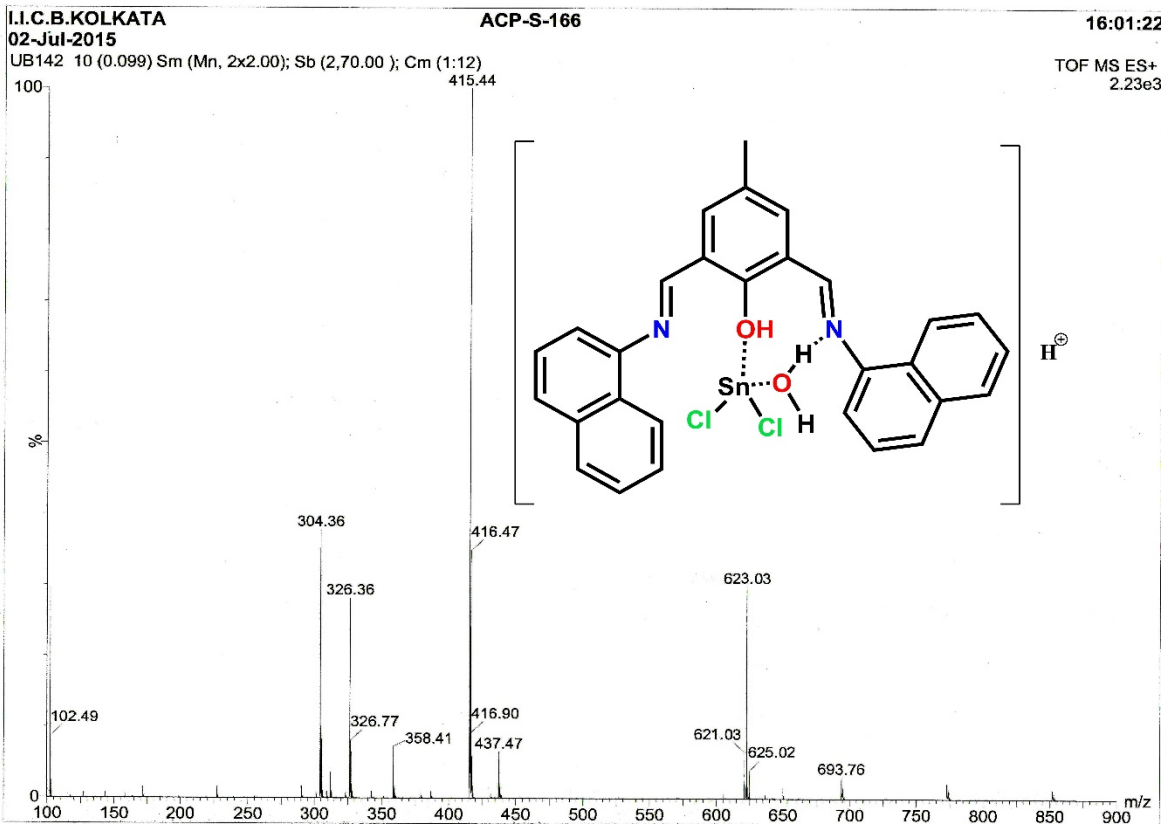

Figure S5. QTOF-MS spectrum of [**L**-$SnCl_2$]complex in MeOH

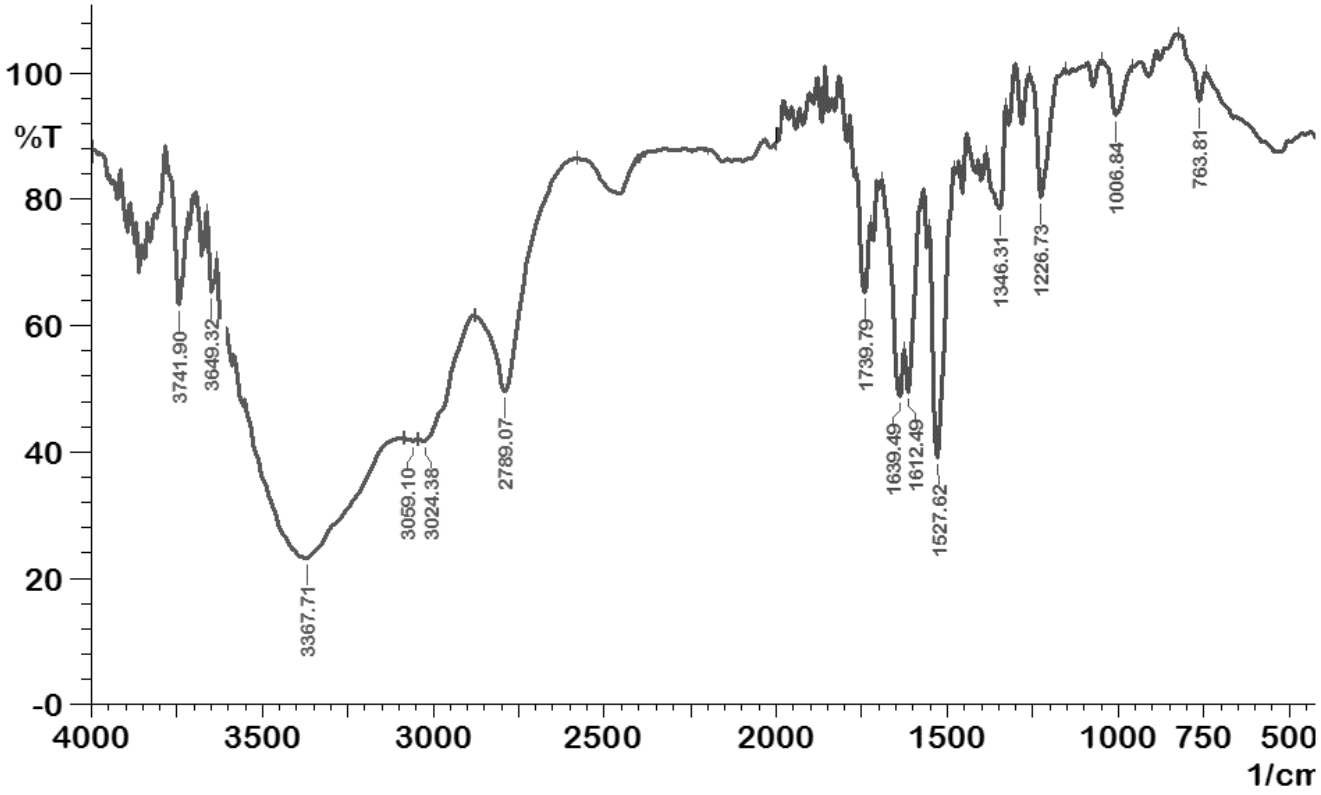

Figure S6. FTIR spectrum of [**L**-$SnCl_2$] complex

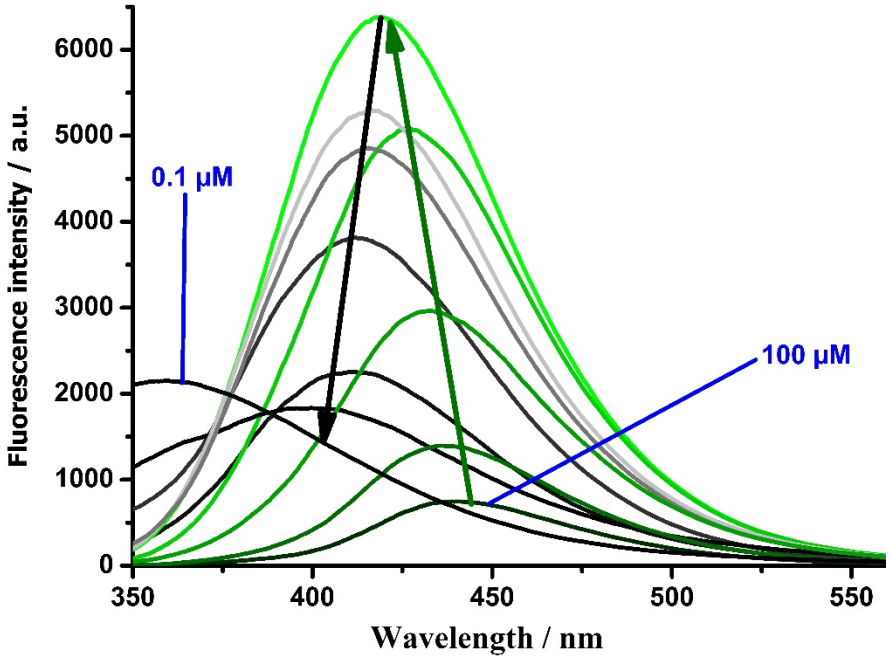

Figure S7. Change of emission spectra of **L** with its concentration (0.1, 0.2, 0.4, 0.75, 1.5, 3.0, 7.5, 10.0, 20.0, 50.0, 100.0 µM in acetonitrile (λ_{ex} = 330 nm).

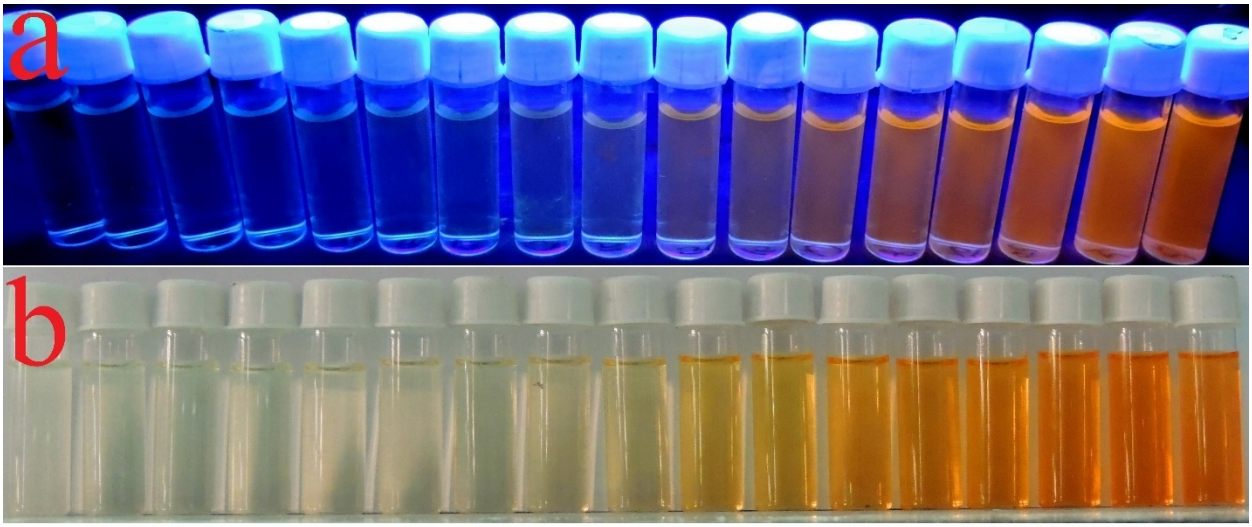

Figure S8. Changes of color of **L** (20 μM) upon addition of Sn^{2+} (0 to 10 equivalent, from left to right) (a) under hand held UV lamp and (b) naked eye in acetonitrile

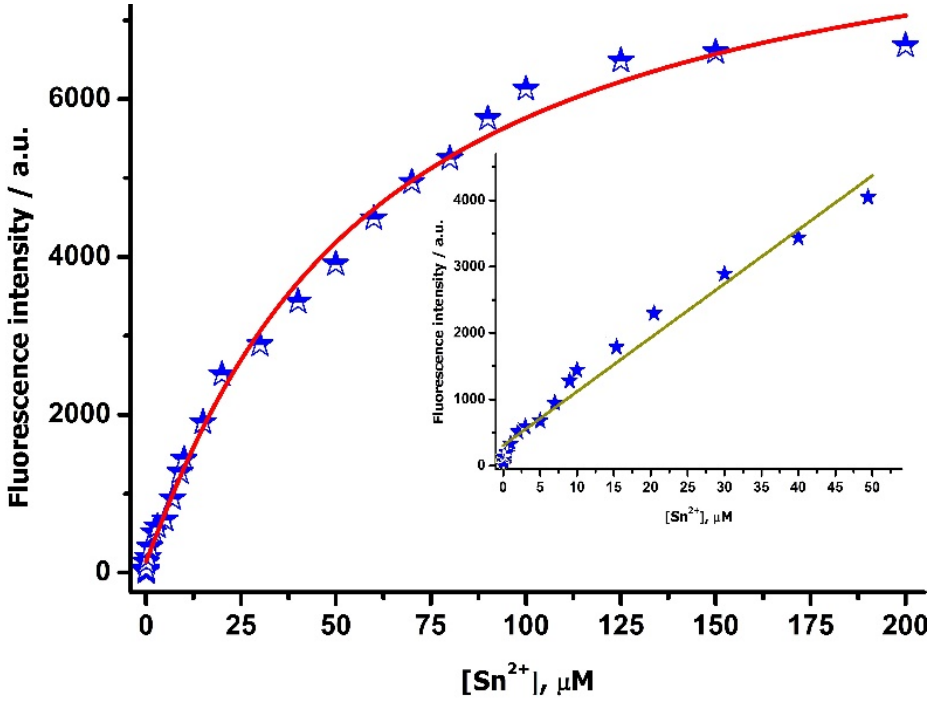

Figure S9. Plot of emission intensity (a.u.) *vs.* Sn^{2+}concentration (μM) at 582mn (λ_{ex}=505 nm). Inset shows the linear region up to 50 μM Sn^{2+} (inset, Slope= 119.06, R^2=0.9899).

Table S1. Comparison of the present probe with those available in the literature

Probe	**LOD**	**Solvent System**	**Interference**	**Additional comment(s)**	**Ref. 15**
R1 and **R2** (Coordination based, turn-on)	R1 = 0.57 μM and R2 = 0.46 μM	ethanol–water (1 : 1, v/v, pH 7.04)	Cu^{2+}, Cr^{3+}	Highly pH sensitive	*Analyst***2014**, *139*, 5223–5229
RBAP (Coordination based, turn-on)	0.044 μM	MeOH/H_2O (2:3, v/v, pH 5.95)	Al^{3+}, Cr^{3+}, Fe^{3+}	Highly pH sensitive	*Molecules* **2014**, *19*, 7817-7831
1o (Coordination based, photochromic)	20.0 μM	Methanol	-	Highly pH sensitive	*Tetrahedron***2014**, *70*, 9070-9076
Present Probe (Coordination based, dynamic to static excimer conversion)	0.01 μM	Acetonitrile	-	can also detect Al^{3+} selectively in 50% aqueous –methanol at different excitation and emission wavelengths	-

Table S2. Fluorescence lifetime decay parameters of **L** and [**L**-$SnCl_2$]complex

λ_{em}		B_1	t_1(ns)	B_2	t_2(ns)	B_3	t_3(ns)	t_{ave}(ns)
420nm	**L**	37.76	0.714	40.42	4.942	21.81	0.0286	2.30
	L+ $SnCl_2$**(10μM)**	16.40	1.535	78.86	6.258	4.74	0.229	5.21
	L+ $SnCl_2$ **(100μM)**	44.85	0.681	40.54	3.318	14.61	0.101	1.67
582nm	**L**	41.42	0.698	27.59	3.166	30.99	0.120	1.20
	L+$SnCl_2$ **(10μM)**	33.28	0.791	51.47	4.527	15.24	0.137	2.61
	L+$SnCl_2$ **(100μM)**	28.47	0.387	71.53	5.389	-	-	3.97

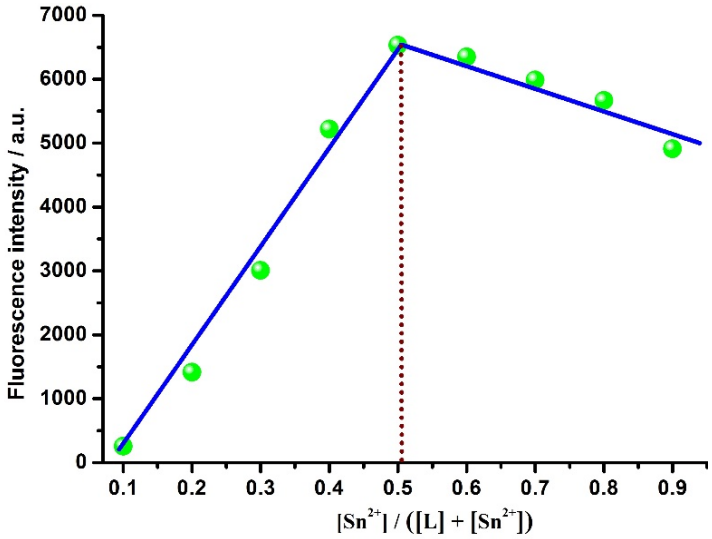

Figure S10. Job's plot for determination of stoichiometry of the [**L**-$SnCl_2$]complex in acetonitrile

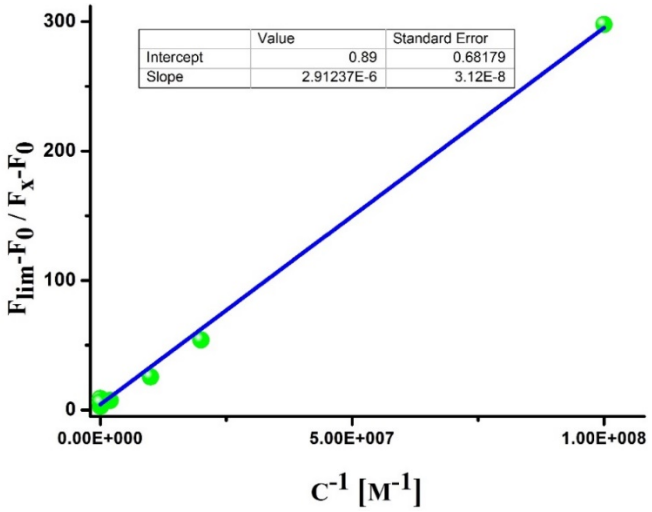

Figure S11. Determination of binding constant of **L** for Sn^{2+} by fluorescence method (R^2=0.89)

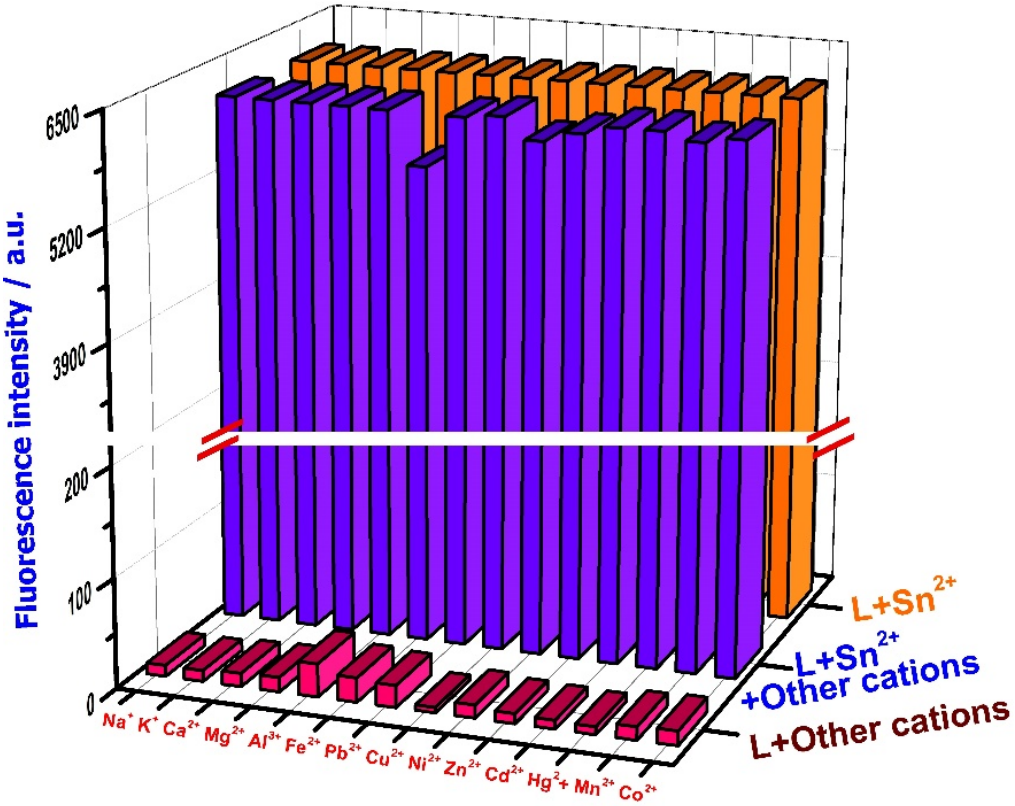

Figure S12. Selectivity of **L** (20 μM) for Sn^{2+} in a competing environment in presence of other cations (100 μM) in acetonitrile,[$SnCl_2$] = 100 μM

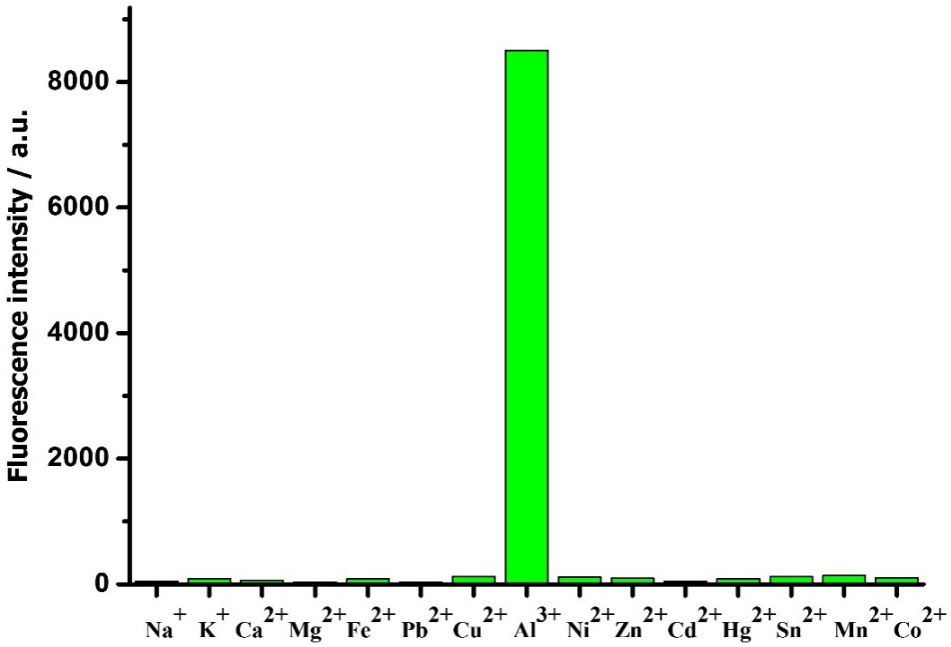

Figure S13. Selectivity of **L** (20 μM) for Al^{3+} (100 μM) in 50% aqueous-methanol (v/v) ([cations] = 100 μM, λ_{ex} = 375 nm, λ_{em} = 501nm)

Table S3. Frontier molecular orbitals (MOs) of **L** and their energy levels (in a.u), Calculations are based on ground state geometry from DFT at B3LYP/3-21G /level using Gaussian 09.

Frontier orbital	Energy (a.u.)	Energy optimized geometry
LUMO	-0.08027	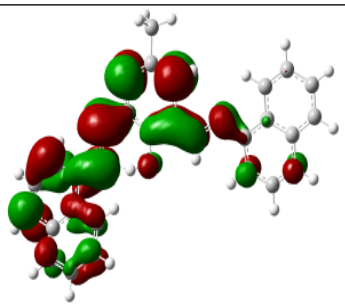
HOMO	-0.19611	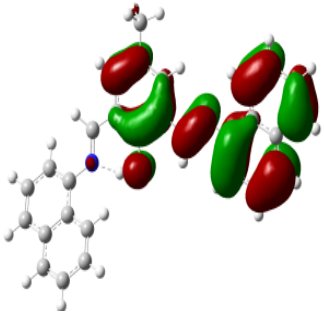

Table S4. Frontier molecular orbitals (MOs) of **L** and their energy levels (in a.u), Calculations are based on ground state geometry using TDDFT at B3LYP/3-21G /level using Gaussian 09.

Frontier orbital	Energy (a.u.)	Energy optimized geometry
LUMO+1	-0.05207	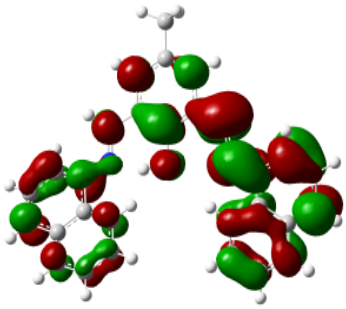
LUMO	-0.07752	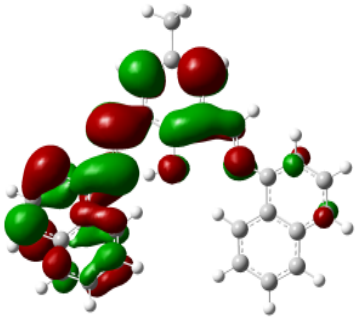
HOMO	-0.19312	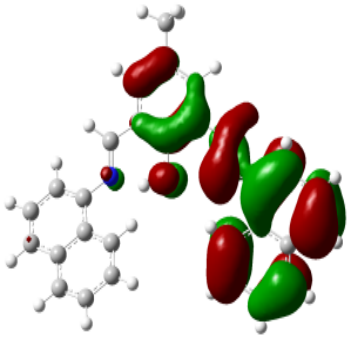
HOMO-1	-0.21052	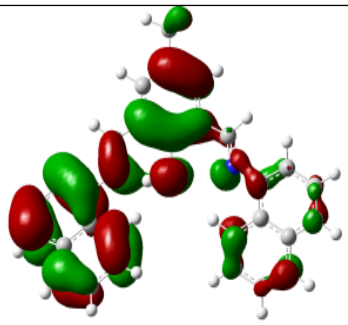

Table S5. Frontier molecular orbitals (MOs) of [**L**-$SnCl_2$]complex and their energy levels (in a.u), Calculations are based on ground state geometry from DFT at B3LYP/6-31G /level using Gaussian 09.

Frontier orbital	Energy (a.u.)	Energy optimized geometry
LUMO+1	-0.09995	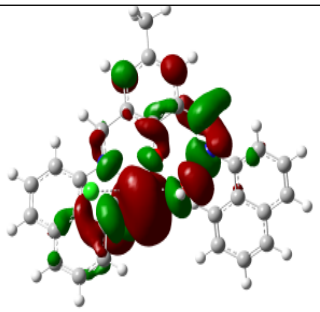
LUMO	-0.12055	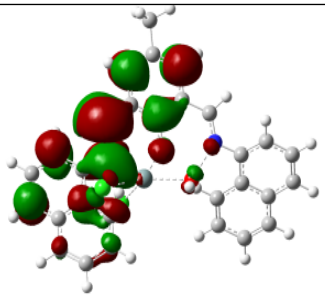
HOMO	-0.1913	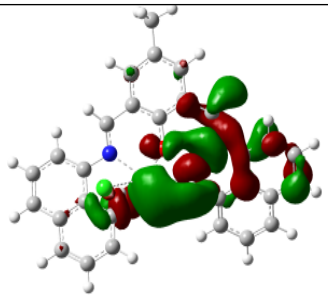
HOMO-1	-0.19554	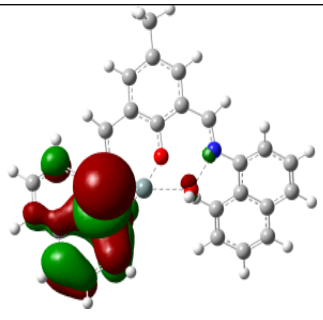

Table S6. Frontier molecular orbitals (MOs) of [**L**-$SnCl_2$] complexand their energy levels (in a. u), Calculations are based on ground state geometry by TDDFT at B3LYP/6-31G /level using Gaussian '09

Frontier orbital	Energy (a.u.)	Energy optimized geometry
LUMO+1	-0.09583	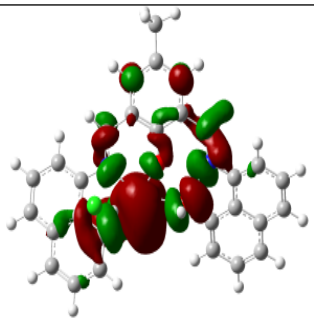
LUMO	-0.17919	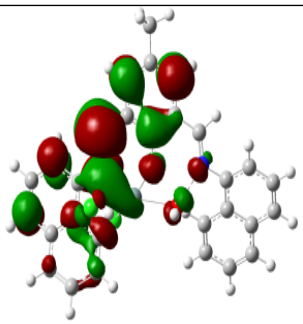
HOMO	-0.20939	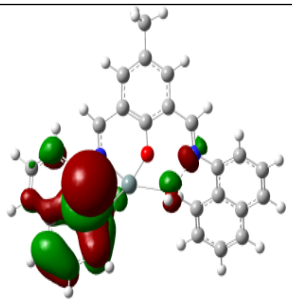
HOMO-1	-0.22437	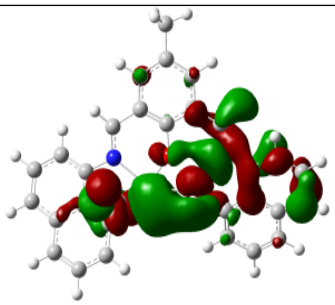

Table S7. Vertical excitation energies (E_{ex}), oscillator strengths (f), and key transitions of thelowest few excited singlets generated from TDDFT calculations for**L** in acetonitrile.

Excitation (eV)	**λ_{ex}(nm)**	**Osc. Strength(f)**	**Key transitions**	**CI**
2.6227 eV	472.74 nm	f =0.6390	HOMO-LUMO	0.62383
2.7489 eV	451.04 nm	f =0.4562	HOMO-1 toLUMO+1	0.27099, 0.61063, 0.16834
2.6575 eV	466.54 nm	f =0.1220	HOMO to LUMO+1	0.28220, 0.18404
2.5421 eV	487.72 nm	f =0.0102	HOMO-2 to LUMO	0.60401, 0.16972
2.4580 eV	504.41 nm	f =0.0946	HOMO to LUMO+2	0.12996, 0.43916, 0.23093

Table S8. Selected bond lengths (Å) and bond angles (°) for **L**

Bond lengths(Å)

O(1)-H(1)	0.82	C(5)-C(33)	1.449(4)	C(9)-C(16)	1.391(5)	C(15)-C(24)	1.360(5)
O(1)-C(3)	1.352(4)	C(6)-C(7)	1.383(5)	C(10)-C(15)	1.402(5)	C(16)-C(27)	1.506(5)
N(3)-C(33)	1.276(4)	C(6)-C(34)	1.462(5)	C(10)-C(18)	1.423(4)	C(17)-H(17)	0.93
N(3)-C(15)	1.427(4)	C(7)-H(7)	0.931	C(10)-C(25)	1.414(5)	C(17)-C(22)	1.372(5)
C(3)-C(5)	1.400(5)	C(7)-C(16)	1.384(5)	C(33)-H(33)	0.929	C(18)-C(20)	1.397(6)
C(3)-C(6)	1.396(4)	C(8)-C(12)	1.421(5)	C(12)-C(14)	1.370(5)	C(18)-C(32)	1.401(6)
N(4)-C(12)	1.420(4)	C(8)-C(17)	1.411(5)	C(34)-H(34)	0.93	C(19)-C(23)	1.416(5)
N(4)-C(34)	1.278(4)	C(8)-C(19)	1.419(5)	C(14)-H(14)	0.93	C(19)-C(30)	1.404(5)
C(5)-C(9)	1.386(5)	C(9)-H(9)	0.929	C(14)-C(21)	1.394(5)	C(20)-H(20)	0.93

C(21)-H(21)	0.929	C(24)-H(24)	0.93	C(27)-H(27A)	0.959	C(30)-H(30)	0.931
C(21)-C(23)	1.360(5)	C(24)-C(31)	1.405(5)	C(27)-H(27B)	0.96	C(31)-H(31)	0.929
C(22)-H(22)	0.929	C(25)-H(25)	0.93	C(27)-H(27C)	0.959	C(31)-C(32)	1.354(6)
C(20)-C(26)	1.353(7)	C(25)-C(28)	1.346(6)	C(28)-H(28)	0.93	C(32)-H(32)	0.929
C(22)-C(29)	1.389(6)	C(26)-H(26)	0.93	C(29)-H(29)	0.928		
C(23)-H(23)	0.929	C(26)-C(28)	1.393(6)	C(29)-C(30)	1.358(7)		

Bond angles(°)		C(3)-C(6)-C(34)	119.6(3)	H(9)-C(9)-C(16)	118.8
H(1)-O(1)-C(3)	109.4	C(7)-C(6)-C(34)	121.3(3)	C(15)-C(10)-C(18)	118.9(3)
C(33)-N(3)-C(15)	118.8(3)	C(6)-C(7)-H(7)	118.5	C(15)-C(10)-C(25)	123.4(3)
O(1)-C(3)-C(5)	121.3(3)	C(6)-C(7)-C(16)	122.9(3)	C(18)-C(10)-C(25)	117.7(3)
O(1)-C(3)-C(6)	118.7(3)			N(3)-C(33)-C(5)	123.3(3)
C(5)-C(3)-C(6)	119.9(3)	H(7)-C(7)-C(16)	118.5	N(3)-C(33)-H(33)	118.3
C(12)-N(4)-C(34)	118.5(3)	C(12)-C(8)-C(17)	122.8(3)	C(5)-C(33)-H(33)	118.4
C(3)-C(5)-C(9)	118.8(3)	C(12)-C(8)-C(19)	119.0(3)	N(4)-C(12)-C(8)	116.9(3)
C(3)-C(5)-C(33)	120.7(3)	C(17)-C(8)-C(19)	118.2(3)		
C(9)-C(5)-C(33)	120.3(3)	C(5)-C(9)-H(9)	118.7	N(4)-C(12)-C(14)	123.2(3)
C(3)-C(6)-C(7)	118.9(3)	C(5)-C(9)-C(16)	122.6(3)	C(8)-C(12)-C(14)	119.8(3)

N(4)-C(34)-C(6)	121.7(3)	C(20)-C(18)-C(32)	121.5(3)	C(15)-C(24)-C(31)	120.9(4)
N(4)-C(34)-H(34)	119.2	C(8)-C(19)-C(23)	118.8(3)	H(24)-C(24)-C(31)	119.5
C(6)-C(34)-H(34)	119.2	C(8)-C(19)-C(30)	119.1(3)	C(10)-C(25)-H(25)	119.7
C(12)-C(14)-H(14)	119.4	C(23)-C(19)-C(30)	122.1(3)	C(10)-C(25)-C(28)	120.6(3)
C(12)-C(14)-C(21)	121.2(3)	C(18)-C(20)-H(20)	119.3	H(25)-C(25)-C(28)	119.7
H(14)-C(14)-C(21)	119.3	C(18)-C(20)-C(26)	121.5(4)	C(20)-C(26)-H(26)	120.4
N(3)-C(15)-C(10)	117.5(3)	H(20)-C(20)-C(26)	119.3	C(20)-C(26)-C(28)	119.2(4)
N(3)-C(15)-C(24)	122.4(3)	C(14)-C(21)-H(21)	119.8	H(26)-C(26)-C(28)	120.4
C(10)-C(15)-C(24)	120.1(3)	C(14)-C(21)-C(23)	120.3(3)	C(16)-C(27)-H(27A)	109.5
C(7)-C(16)-C(9)	116.8(3)	H(21)-C(21)-C(23)	119.9	C(16)-C(27)-H(27B)	109.4
C(7)-C(16)-C(27)	122.2(3)	C(17)-C(22)-H(22)	119.8	C(16)-C(27)-H(27C)	109.4
C(9)-C(16)-C(27)	121.0(3)	C(17)-C(22)-C(29)	120.4(4)	H(27A)-C(27)-H(27B)	109.4
C(8)-C(17)-H(17)	119.6	H(22)-C(22)-C(29)	119.7	H(27A)-C(27)-H(27C)	109.6
C(8)-C(17)-C(22)	120.9(3)	C(19)-C(23)-C(21)	120.8(3)	H(27B)-C(27)-H(27C)	109.5
H(17)-C(17)-C(22)	119.6	C(19)-C(23)-H(23)	119.6	C(25)-C(28)-C(26)	121.7(4)
C(10)-C(18)-C(20)	119.2(3)	C(21)-C(23)-H(23)	119.6	C(25)-C(28)-H(28)	119.1
C(10)-C(18)-C(32)	119.4(3)	C(15)-C(24)-H(24)	119.6	C(26)-C(28)-H(28)	119.2

C(22)-C(29)-H(29)	119.9	C(19)-C(30)-H(30)	119.3	H(31)-C(31)-C(32)	119.8
C(22)-C(29)-C(30)	120.2(4)	C(29)-C(30)-H(30)	119.5	C(18)-C(32)-C(31)	120.4(4)
H(29)-C(29)-C(30)	119.8	C(24)-C(31)-H(31)	119.9	C(18)-C(32)-H(32)	119.8
C(19)-C(30)-C(29)	121.2(4)	C(24)-C(31)-C(32)	120.3(4)	C(31)-C(32)-H(32)	119.8

Table S8. Selected crystal parameters of **L**

Empirical formula	C_{29} H_{22} N_2 O
Formula weight	414.49
Temperature	296 K
Wavelength	0.71073 Å
Crystal system	Monoclinic
Space group	$P2_1/c$
Unit cell dimensions	a = 17.662(10) Å, b = 16.526(9) Å, c = 7.599(4) Å
	α = 90°, β = 97.592(9)°, γ = 90°
Volume	2199(2) $Å^3$
Density	1.252 g cm^{-3}
Z	4
F(000)	872.0
Theta (max)	25.360°
Index ranges	-21<=h<=21, -19<=k<=19, -9<=l<=9
Data completeness	0.980
R indices (all data)	R1 = 0.0650, wR2 = 0.2140